Solid State Nuclear Magnetic Resonance 107 (2020) 101660

Contents lists available at ScienceDirect

Solid State Nuclear Magnetic Resonance

journal homepage: www.elsevier.com/locate/ssnmr

Trends

Solid-state NMR of plant and fungal cell walls: A critical review

Wancheng Zhao, Liyanage D. Fernando, Alex Kirui, Fabien Deligey, Tuo Wang *

Department of Chemistry, Louisiana State University, Baton Rouge, LA, 70803, USA

ARTICLE INFO

Keywords:
Solid-state NMR
DNP
Cell wall
Plant
Fungi
Carbohydrate
Polysaccharides
Cellulose
Lignin
Xylan

ABSTRACT

The cell walls of plants and microbes are a central source for bio-renewable energy and the major targets of antibiotics and antifungal agents. It is highly challenging to determine the molecular structure of complex carbohydrates, protein and lignin, and their supramolecular assembly in intact cell walls. This article selectively highlights the recent breakthroughs that employ $^{13}C/^{15}N$ solid-state NMR techniques to elucidate the architecture of fungal cell walls in *Aspergillus fumigatus* and the primary and secondary cell walls in a large variety of plant species such as *Arabidopsis*, *Brachypodium*, maize, and spruce. Built upon these pioneering studies, we further summarize the underexplored aspects of fungal and plant cell walls. The new research opportunities introduced by innovative methods, such as the detection of proton and quadrupolar nuclei on ultrahigh-field magnets and under fast magic-angle spinning, paramagnetic probes, natural-abundance DNP, and software development, are also critically discussed.

1. Cell walls: a medically important and energy-relevant biomaterial

The cell wall is a carbohydrate-rich coating outside the plasma membrane of plants and many microorganisms. The cell walls in photosynthesis systems, such as plants, algae, and green bacteria, are transformed from solar energies and carbon dioxide, with enormous value as a primary source of building materials, textiles, biofuel, nanocomposites, and high-value reagents [1]. Polysaccharides in the cell walls of fungal pathogens and invading bacteria are absent in human cells; these components trigger immune recognition and serve as the major target of antifungal drugs and antibiotics [2,3]. Polysaccharides and other biomolecules (such as protein and lignin) are held together by covalent linkages and physical packing interactions to form a mechanically strong composite, which allows the cell to retain integrity and morphology under external stress. Nevertheless, the numerous interactions between biopolymers also pose a challenge for post-harvest processing and utilization of biomass and make it technically difficult to characterize these biomaterials with high resolution.

Recently, magic-angle-spinning (MAS) solid-state NMR spectroscopy has been extensively employed to investigate intact cell walls. Uniformly isotope-labeled samples are produced by feeding the organism of interest with $^{13}CO_2$ or solid/liquid media containing ^{13}C-glucose and ^{15}N-salts [4]. Multidimensional ^{13}C–$^{13}C/^{15}N$ correlation spectra collected on whole cells or isolated cell walls provide the atomic resolution needed for determining the polymorphic structure, intermolecular interaction, water contact, and molecular motions of biomolecules in their cellular environment (Fig. 1). Within the last decade, a large variety of biosystems have been studied: the primary and secondary cell walls of seven plant species, including *Arabidopsis thaliana, Brachypodium distachyon* and *Zea mays* (maize), rice, switchgrass, poplar and spruce [5–14]; the biofilm or cell walls of bacterial and fungal pathogens such as *Aspergillus fumigatus*, *Cryptococcus neoformans*, and *Bacillus subtilis* [15–21]; as well as the carbohydrate components in microalgae *Chlamydomonas reinhardtii* [22]. Here we will review the major findings related to plant and fungal cell walls, emphasize the key questions awaiting investigation, and discuss the future directions enabled by the improved instrumentation and methodology, in the attempt to inspire innovative research in carbohydrate and cell wall NMR.

2. Recent advances in cell wall research by solid-state NMR

2.1. Molecular insight of plant primary cell walls

Since 2010, Hong and colleagues have been pioneering the investigations of primary plant cell walls, a component synthesized in the growing plants (Fig. 2a–c) [23,24]. The composition is well known from numerous biochemical studies, and three major types of polysaccharides are present [25,26]. Cellulose microfibrils are formed by 18 or more glucan chains (3–4 nm across) and they are highly rigid and partially

* Corresponding author.
E-mail address: tuowang@lsu.edu (T. Wang).

https://doi.org/10.1016/j.ssnmr.2020.101660
Received 15 February 2020; Accepted 17 March 2020
Available online 26 March 2020

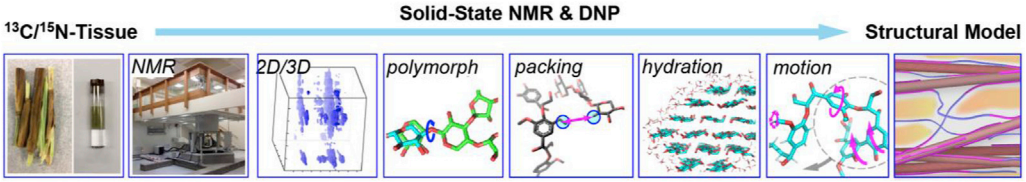

Fig. 1. Solid-state NMR strategy for investigating cell wall materials.

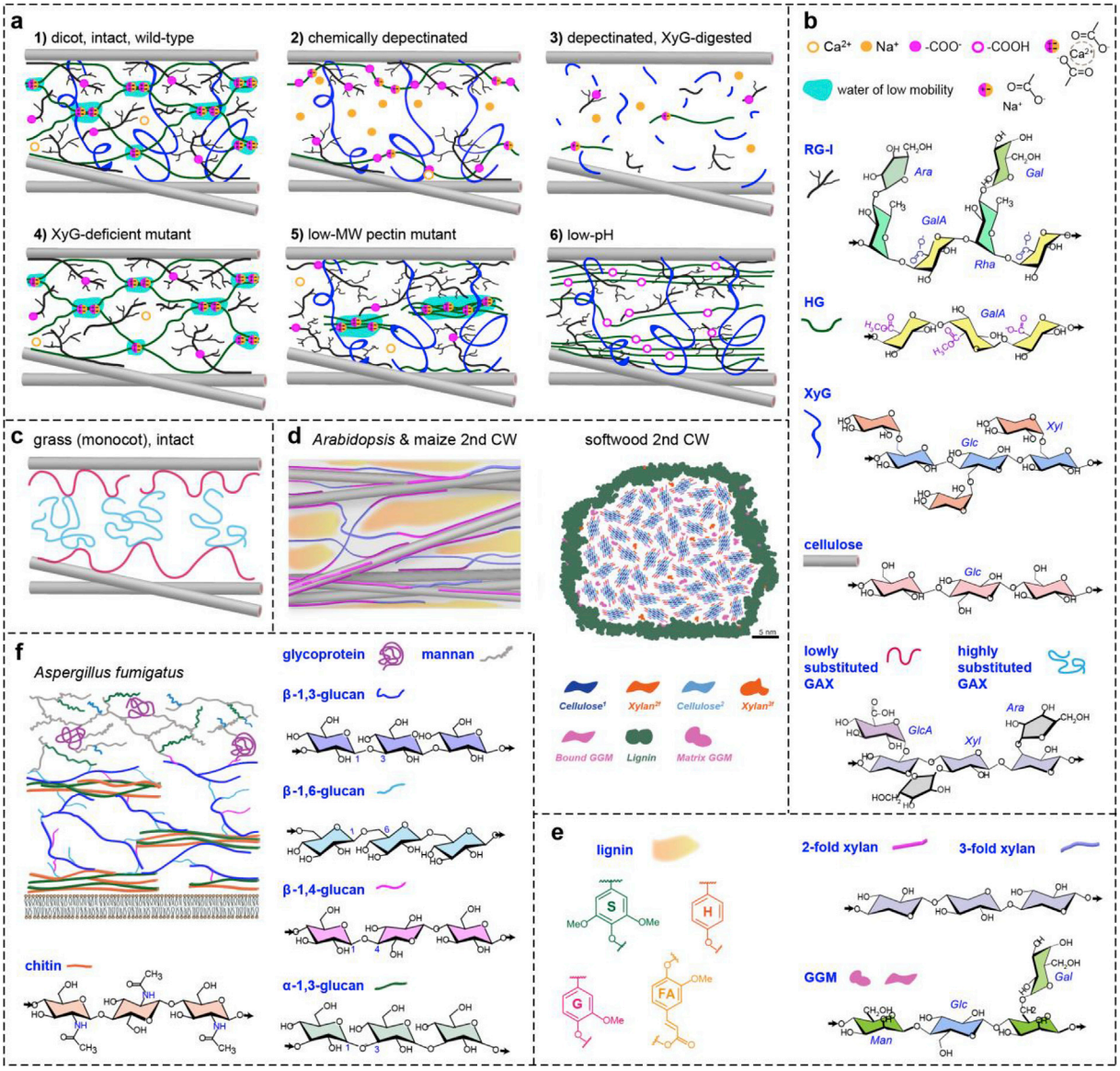

Fig. 2. Cell walls and biomolecules studied by solid-state NMR. **a**, NMR-derived conceptual models of primary cell walls of *Arabidopsis* (dicot), including the intact and wild-type cell walls at different pH values, as well as multiple mutants that attenuate the structure and content of matrix polysaccharides (pectin or XyG), sequentially digested cell walls that are chemically depectinated followed by enzymatical removal of XyG. The sample numbers are labeled to facilitate discussion. **b**, Chemical structures of the biomolecular components in primary plant cell walls. **c**, Structural scheme of primary grass cell walls based on data collected using *Brachypodium* and maize. **d**, Plant secondary (2nd) cell wall architecture of *Arabidopsis*, maize, and the softwood spruce. **e**, Representative structure of polymers that are unique to secondary plant cell walls. **f**, the structure and polymers of fungal cell walls in *A. fumigatus*. Adapted from reference [5,8,13,15,29,30,32,33,35] with copyright permission.

crystalline. The backbones of pectin, such as rhamnogalacturonan-I (RG-I) and homogalacturonan (HG), are often acidic and responsible for regulating cell wall hydration. Hemicellulose interacts with cellulose and pectin, with a plant-dependent composition: the major hemicellulose in primary cell walls is xyloglucan (XyG) in dicots, such as *Arabidopsis*, but changes to glucuronoarabinoxylan (GAX) and mixed-linkage glucans (MLG) in commelinid monocots (grasses) such as *Brachypodium* and maize. Using ^{13}C-labeled and isolated cell walls, three ground-breaking discoveries were reported, which have revised and substantiated our limited understanding of primary cell wall architecture.

First, cellulose, hemicellulose, and pectin are found to associate noncovalently on the sub-nanometer scale to form an integrated network. In wild-type *Arabidopsis* (Fig. 2a, Sample 1), a large number of cross peaks have been identified between pectin and cellulose, which were previously considered to be phase-separated [5]. The equilibrium intensity of ^{13}C–^{13}C spin diffusion suggests that 25–50% of cellulose are in close proximity to pectin [6,27]. This polymer interaction is independent of the sample's hydration history [28] and can be fully preserved after partial depectination by CDTA and sodium carbonate (Fig. 2a, Sample 2), which disrupts the calcium crosslinking of HG and consequently removing the interfibrillar HG molecules (40% of all HG) that are not binding cellulose [28–30]. Due to the loss of immobilized water in the depectinated sample, the rate of ^{1}H–^{1}H polarization transfer from water to polymers have been globally slowed down for all polysaccharides, which can be partially restored by the subsequent digestions of XyG using xyloglucanase and Cel12A enzymes due to the enhanced surface areas of the residual macromolecules (Fig. 2a, Sample 3) [29]. In addition, the removal of XyG using an *xxt1xxt2xxt5* triple knockout line (Fig. 2a, Sample 4) markedly enhances the dynamics of the remaining polysaccharides [5], which echoes with the global alternation of ^{1}H spin diffusion observed in the sequentially digested samples, revealing a single network of all polysaccharides.

It is noteworthy that a weaker pectin-cellulose interaction is often accompanied by the chemical modification of pectin structure, for example, a higher degree of methyl esterification, an increased occurrence of sidechain branching by arabinan or galactan, a reduced extent of calcium-crosslinking, and promoted HG aggregation. These molecular changes macroscopically correlate with faster growth, for example, in the inflorescence stem of *Arabidopsis* with a segmentally increasing rate of elongation from the base to the apical region (the tip) [31], in the $PGX1^{AT}$ mutant that produces smaller pectin but larger plants (Fig. 2a, Sample 5) [32], and in a low-pH sample that mimics the acid growth condition (Fig. 2a, Sample 6) [33].

Second, with the assistance from Dynamic Nuclear Polarization (DNP) and paramagnetic methods, two methods have been developed to reveal how a class of proteins (expansin) unfasten the polysaccharide joints to mediate cell expansion [34,35]. Expansins lack the lytic activity expected for wall-loosening enzyme and have been assumed to disrupt the non-covalent contacts between polysaccharides [36]. Solid-state NMR studies have shown that expansins perturb the cellulose-xyloglucan nexus in *Arabidopsis* but disrupt the junctions between the highly and lowly substituted GAX in maize (Fig. 2c); therefore, expansins bind different polysaccharides in the cell walls with distinct composition.

Third, with the sharp ^{13}C linewidths on high magnetic fields (0.7–1.0 ppm for cellulose on an 800 MHz NMR) and the chemical shift calculations using Density Functional Theory (DFT), we have resolved seven types of glucose units in the cellulose of *Arabidopsis* and grass primary cell walls, determined their hydroxymethyl conformations via ^{1}H–^{1}H distance measurement, and localized these conformers in the microfibrils [37–39]. These forms deviate noticeably from the crystallographic structures of Iα and Iβ allomorphs obtained using the highly crystalline cellulose from bacteria and tunicates (a marine animal). In addition, these seven types of glucose residues have been consistently observed in the secondary cell walls of *Arabidopsis*, maize, switchgrass, and rice [8], as well as multiple woody plants such as *Eucalyptus*, poplar, and spruce (unpublished results). Therefore, the Iα and Iβ model allomorphs are generally absent in most natural resources. So far, the NMR signals of Iα and Iβ structures have only been observed in cotton, thus a large crystallite is a prerequisite for accommodating the model structures [40].

2.2. Lignin-carbohydrate packing in plant secondary cell walls

The secondary cell wall is formed once the cell ceases expansion and it comprises the majority of lignocellulosic biomass. In secondary cell walls, cellulose microfibrils aggregate into larger bundles (10–20 nm across), which are further embedded in a matrix containing the aromatic polymer lignin and hemicellulose such as xylan and glucomannan [41]. Lignin-carbohydrate interactions confer the biomass with recalcitrance to chemical and enzymatical treatments; therefore, it is of broad interest to understand the chemical principles underlying these polymer interactions. Paul Dupree, Ray Dupree, and colleagues have conducted several studies to recognize the functional relevance of xylan polymorphism in *Arabidopsis* secondary cell walls. It is found that only the xylan with a 2-fold helical screw symmetry and a regular pattern of acetate or glucuronate substitutions can bind cellulose microfibrils [10–12].

Stimulated by these discoveries, we have investigated the mature stems of maize, rice, switchgrass, and *Arabidopsis*, using a series of $2D^{13}C$–^{13}C correlation methods specially designed for enhancing the aromatic signals of lignin and detecting the lignin-carbohydrate interface (Fig. 3a) [8]. Hundreds (234) of intermolecular cross-peaks have been identified, which pinpoint six categories of packing interactions between the different functional groups in lignin and carbohydrates as illustrated in Fig. 3b-g. Strikingly, lignin mainly interacts with xylan rather than cellulose. In addition, the number and intensities of these cross peaks statistically correlate with the number of methyl ether substitutions in lignin residues (Fig. 3b), which signposts a prevalent role of electrostatic contacts in stabilizing polymer interface. Integrating the information on polymer packing, dynamics, and hydration has resulted in a molecular view of lignocellulosic materials: lignin self-aggregates to form dynamically unique and hydrophobic nanodomains, with surface contact to the non-flat xylan (3-fold) through abundant electrostatic interactions [8]. This xylan-lignin interface links to the flat-ribbon domain of xylan that is coating the surface of cellulose microfibrils (Fig. 2d, left).

In the softwood spruce, xylan also binds cellulose through its 2-fold conformer while galactoglucomannan (GGM), a unique hemicellulose in softwoods, binds the surface of cellulose microfibrils in a semi-crystalline manner [13]. Since both GGM and xylan have shown two domains, one coating cellulose and the other filling interfibrillar space, it is proposed that some GGM and xylan bind to the same microfibril and further associate with lignin (Fig. 2d, right).

2.3. Insights into the fungal cell wall architecture

Recently, we have also initiated a project elucidating the cell wall structure of an airborne fungal pathogen *A. fumigatus*. The samples are measured alive at room-temperature on an 800 MHz NMR; the ^{13}C linewidths are as narrow as 0.4–0.6 ppm for the rigid polysaccharides and 0.3–0.5 ppm for the relatively mobile carbohydrates and proteins. With the remarkable resolution, the ^{13}C and ^{15}N signals of 7 types of polysaccharides, including α-1,3-glucan, chitin (a nitrogenated polysaccharide), mannan, and three types of β-glucans, together with their 23 conformers, have been identified (Fig. 2f) [15]. Long-range correlation methods, such as ^{13}C–^{13}C and ^{15}N–^{15}N Proton-Assisted Recoupling (PAR) [42] as well as NCACX measured with a variable ^{13}C–^{13}C mixing time, have been employed to identify in total 65 intermolecular interactions. Most of these physical interactions occur between chitin and α-1,3-glucans (Fig. 4a), which also show high hydrophobicity (Fig. 4b and c) and rigidity. These two molecules are complexed to form a mechanical scaffold that is surrounded by a soft matrix of diversely linked β-glucans and capped by an external shell rich in glycoproteins (Fig. 2f). This study has established a preliminary structural frame, which requires systematic validation and encourages structural investigations of individual cell wall molecules and their biomedical relevance.

3. Biochemical perspectives: the unresolved questions

In an earlier Trends article published in 2016, several underexplored areas in plant NMR have been summarized, which mainly include the coalescence of multiple cellulose microfibrils, the functional structure of lignin, and the putative interactions between polysaccharides and

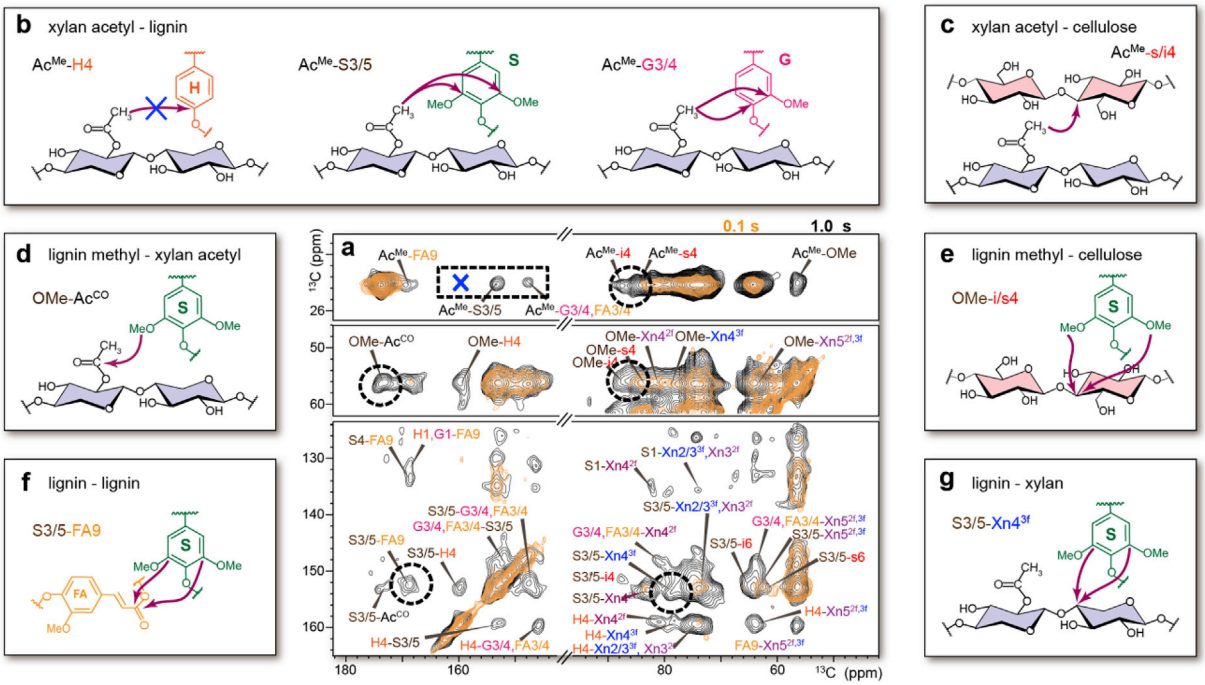

Fig. 3. Intermolecular interactions in plant secondary cell walls by dipolar-filtered PDSD spectra. **a**, Overlay of 2D^{13}C–^{13}C correlation spectra measured with a short (0.1 s, yellow) and long (1.0 s, black) mixing time on maize stems. Six representative regions of intermolecular cross peaks for the structural illustration in panels **b-g** are highlighted in dashline circles or rectangle. These interactions happen between **b**, xylan acetyl (Ac) group and lignin aromatics (S, G, or H), **c**, xylan acetyl group and cellulose microfibrils (i: internal glucan chains; s: surface chains), **d**, lignin methyl group (OMe: methyl ether) and xylan acetyl groups, **e**, lignin methyl group and cellulose, **f**, the aromatic carbons of different lignin units, as well as **g**, lignin aromatics and xylan furanose ring. The blue crosses in panels **a** and **b** highlight the missing signal of Ac^{Me}-H4 cross peak between xylan and the H-residue of lignin. Adapted from reference [8] with copyright permission.

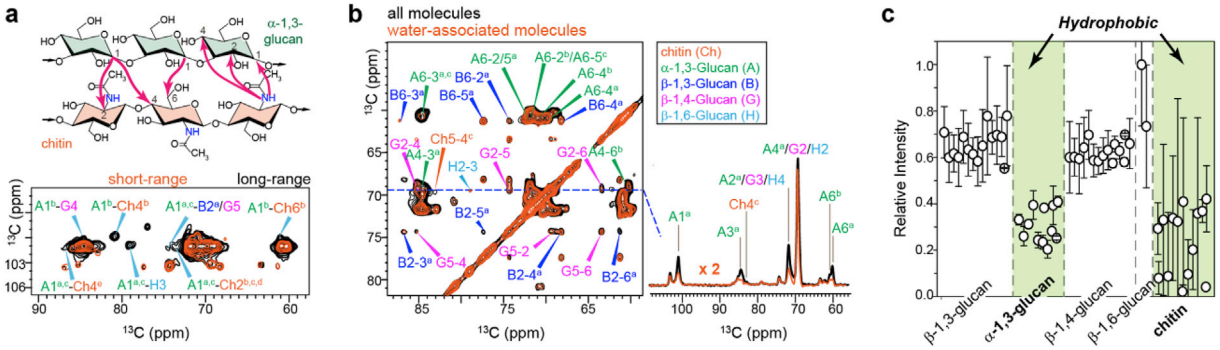

Fig. 4. Polymer packing and hydration in fungal cell walls of *A. fumigatus*. a, Top: Illustration of the observed cross peaks between α-1,3-glucan (A) and chitin (Ch). Bottom: overlay of 2D^{13}C–^{13}C correlation spectra measured with 100 ms DARR (orange, short-range) and 15 ms PAR (black, long-range). **b**, Overlay of the control (black) and water-edited spectra (orange); the cross section extracted at 69 ppm shows apparent signal dephasing of chitin and α-1,3-glucan in water-edited spectra. **c** Site-specific hydration map of biopolymers. Adapted from reference [15] with copyright permission.

structural proteins [24]. So far, we have already obtained an in-depth understanding of lignin-carbohydrate interactions in secondary cell walls but also discovered more aspects that remain ambiguous. For instance, the sophisticated patterns of covalent linkages between lignin residues and their impact on lignin's capability of interacting with polysaccharides have not been discussed. Cellulose-lignin interaction is scarce in maize and *Arabidopsis*, but this concept may not hold for the woody plants with a distinct composition of biomolecules and a more compact packing. The conformational relevance of glucomannan in spruce and other softwood species is not yet understood. We also need to understand the structural origin of the abundant electrostatic interactions between carbohydrates and aromatics and how these physical contacts contribute to the mechanical properties and digestibility of lignocellulosic materials. Inevitably, we also need to figure out a way to integrate solid-state NMR results with the numerous studies using solution-NMR, which are focused on the covalent linkages in extracted residuals.

An unexpected finding in the *A. fumigatus* fungus is the multifaced role of α-1,3-glucans. These molecules are simultaneously in association with chitin for stiffness and existing in the mobile phase [15]. This observation has countered the biochemical results in which α-1,3-glucans are extractable by strong alkali and thus constantly excluded from the structural core of any prevailing models [43]. Also, the amount of this polysaccharide is much lower in many other pathogens such as most yeasts (for example, *Candida albicans*); therefore, it is of great interest to understand the structural and dynamical heterogeneity of

polysaccharides across fungal species. Another major polysaccharide, mannan, is found to coexist with proteins in the mobile domain of *A. fumigatus* cell walls, likely constituting the mannoproteins in the outermost layer as depicted in biochemical studies. Further evidence assessing the structural role of mannan and their covalent linkages with structural proteins are crucial to the understanding of this structurally dynamic shell that regulates cellular recognition and fungal pathogenesis [44]. It is also important to understand how the microbe re-structures its cell wall in response to antifungal agents, which will explain the origin of drug resistance from a structural perspective.

4. Technical outlook: opportunities beyond conventional methods

The past decade has seen the rapid development of solid-state NMR techniques. Here, we have selectively summarized a few technical advances that could potentially revolutionize the field and establish new research directions. These highlights have extended beyond the conventional $^{13}C/^{15}N$-methods by involving other NMR-active nuclei or electrons, with assistance from ultra-fast MAS, ultrahigh magnetic field, DNP, as well as database and software coding.

4.1. ^{1}H and ^{19}F under fast spinning: carbohydrate structure and interactions

Direct detection of proton resonance provides high-sensitivity due to the high isotope abundance (99.985%) and four-fold higher gyromagnetic ratio over ^{13}C. The strong homonuclear couplings enable distance measurement beyond 1 nm and facilitate structural determination. Although proton detection has already been widely employed to study perdeuterated or protonated proteins [45–48], it is rarely applied to the carbohydrates that are rich in protons with complex chemical environments. Recently, Hong and Phyo have conducted a set of proton-detection experiments, such as the 2D CH INEPT, 3D CHH INEPT-TOCSY, and 2D hChH RFDR techniques [49–51], to assign the ^{1}H resonances of polysaccharides and to determine their intermolecular packing, for example, through cross peaks between cellulose carbons and matrix polysaccharide protons, in ^{13}C-labeled *Arabidopsis* primary cell walls [52]. The protonated material has been back exchanged in D_2O, which suppresses the water intensities and reduces the contribution of hydroxyl protons. A moderately fast MAS frequency (30–50 kHz) is chosen to simultaneously enable proton-detection of the mobile matrix and filter out the signals of rigid microfibrils [52]. The narrow ^{1}H linewidth (0.06 ppm on an 800 MHz spectrometer, Fig. 5a) and the excellent agreement between solid-state ^{1}H chemical shifts and solution-NMR observables consistently confirmed that the observed matrix polysaccharides are intrinsically mobile in cell walls. In addition, Simorre, Schanda, and coworkers have assigned the resonances of peptidoglycan in intact *Bacillus subtilis* under 100 kHz MAS, with representative ^{1}H linewidths of 50–120 Hz (0.05–0.13 ppm) on a 950 MHz spectrometer [53,54]. Using the ^{1}H–^{1}H RFDR scheme, the authors have identified multiple inter-residue cross peaks, including unambiguous cross peaks between the GlcNAc sugar and the L-alanine residue on the peptide stem, crossing a long distance of at least 5 Å [53]. These studies have presented a novel strategy for investigating complex biosystems and landed the stage for pursuing ^{1}H investigations without labeling.

Similarly, ^{19}F has a high gyromagnetic ratio and 100% natural abundance. Adding to these merits is a large range of chemical shifts

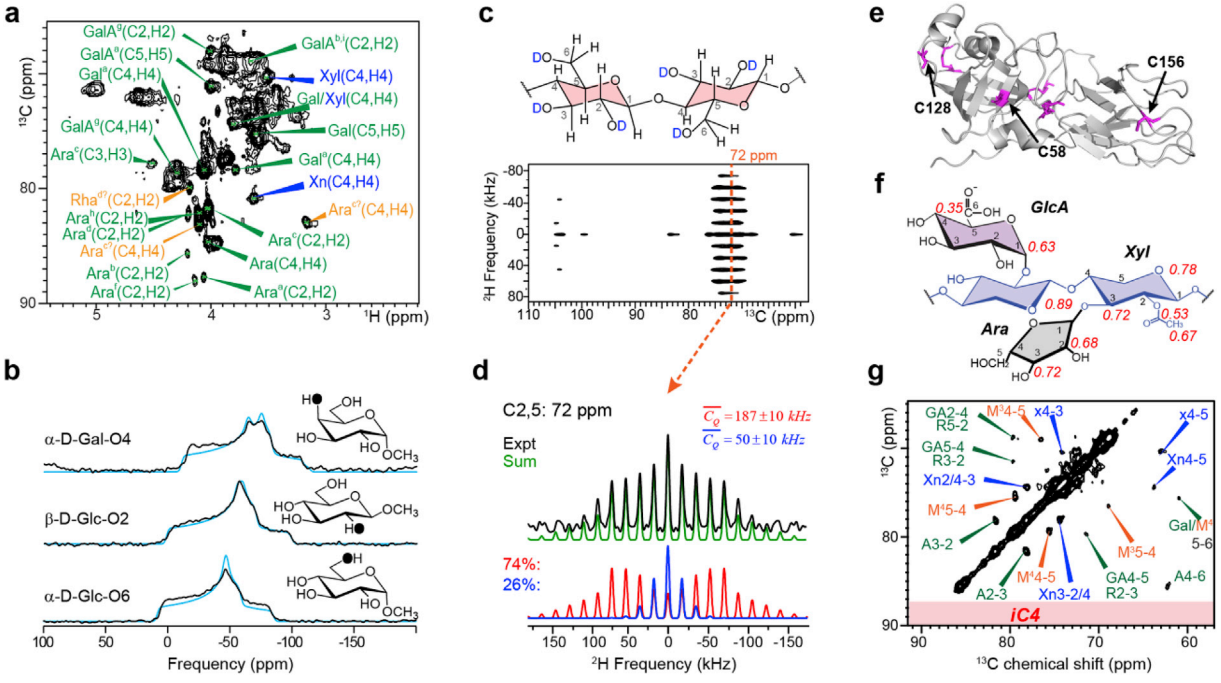

Fig. 5. Advanced techniques that promote carbohydrate and cell wall research. **a**, 2D CH INEPT spectrum of ^{13}C labeled *Arabidopsis* cell walls measured at 50 kHz MAS on an 800 MHz NMR. Superscripts denote the different subtypes of monosaccharides and ambiguous assignments are shown in orange. **b**, Experimental (black) and simulated (blue) ^{17}O MAS spectra at 19.6 T of methyl α-D-galactopyranoside (4-^{17}O), methyl β-D-glucopyranoside (2-^{17}O), and methyl α-D-glucopyranoside (6-^{17}O) at 12 kHz MAS. **c**, 2D ^{2}H–^{13}C correlation spectrum of H/D exchanged and ^{13}C-labeled *Arabidopsis* cell wall. The structure of cellulose and ^{2}H-exchanged OD sites are given. **d**, The 72-ppm ^{2}H cross-sections (black) and best-fit simulation (green) that is a supercomposition of components with C_Q values of 187 and 50 kHz with weighting factors of 74 and 26%, respectively. **e**, The structure of β-expansin (EXPB1) with 9 Cys residues shown in magenta. The 3 solvent-accessible cysteines that could be tagged with EDTA-Mn(II) are annotated. **f**, The PRE effect of Mn(II)-tagged expansin on glucuronoarabinoxylan (GAX). The intensities ratios of 2 spectra measured on the Mn-containing sample and the control sample are shown in red: GAX has significant signal dephasing due to binding to the protein. **g**, Difference PDSD spectrum of two parent spectra measured on Mn-containing or Mn-free samples: showing no cellulose intensities (iC4) but only the signals of matrix polysaccharides that bind proteins. Adapted from reference [35,52,63,70] with copyright permission.

for resolving various chemical motifs. As demonstrated on pharmaceutical compounds, GB1 protein, and HIV-1 capsid protein, ^{19}F–$^{19}F/^{1}H$ distances can be measured on the nanometer scale (1–2 nm) [55–57], which is a major extension from the reach of ^{13}C and ^{15}N methods. Typically, site-specific fluorination causes minimal perturbation to the structures of many proteins and materials [56,58], but may substantially disrupt the hydrogen bonds in carbohydrate polymers. An appropriate labeling scheme is needed to sparsely fluorinate carbohydrates without eliminating their functional structures and assembly [59].

4.2. ^{17}O at ultrahigh-field: a new biochemical probe

Oxygen is another core element that determines the hydrogen bonding and chemical properties of biomolecules. Carbohydrates are particularly rich in oxygen atoms, with at least one oxygen covalently linked to each single carbon site. Recently, the materialization of a world-record 1.5 GHz (35 T) series-connected hybrid (SCH) NMR magnet [60] and the commercial ultrahigh field instruments have presented a unique opportunity for high-resolution ^{17}O studies. Griffin and colleagues have revealed the markedly improved resolution of ^{17}O spectra on ultrahigh fields where the line-broadening by second-order quadrupole coupling is attenuated [61]. They have also collected $2D^{13}C/^{15}N/^{1}H$–^{17}O correlation spectra and determined internuclear distances through recoupling methods such as ZF-TEDOR and REAPDOR [61,62]. Back in 2007, Grandinetti and coworkers have already pioneered the measurement of ^{17}O MAS patterns for monosaccharides and disaccharides that are site-specifically labeled at either the hydroxyl or glycosidic oxygen sites (Fig. 5b) [63]. The C–O–H angle and C–O distances, instead of the O–H distances, are found to affect ^{17}O quadrupolar couplings in carbohydrates. In addition, many other quadrupolar nuclei may benefit from the availability of ultrahigh-field magnets. For example, ^{33}S NMR could help characterize many sulfurated carbohydrates (such as the ulvan, carrageenan, and rhamnan sulfate) in marine species [64]. Another popular molecule is heparin, a sulfated glycosaminoglycan that prevents blood clotting as an anticoagulant agent and induces filament assembly of tau proteins [65]. Combining quadrupolar NMR with ultrahigh field magnets provides a novel probe to the biochemically important sites in these carbohydrates but improved methods are needed for resolving the many oxygen sites in biological samples.

4.3. ^{2}H: dynamics and water accessibility

In cell walls, carbohydrate dynamics were primarily evaluated by measuring NMR relaxation and dipolar couplings [66], and water-polymer contacts were mainly investigated using $1D/2D^{13}C$-detected, ^{1}H spin diffusion methods and dipolar-filtered heteronuclear 2D correlation techniques like MELODI-HETCOR [28,29,67] Recently, Hong and coworkers have employed the Rotor Echo Short Pulse IRrAdiaTION mediated cross-polarization ($^{RESPIRATION}CP$) technique [68,69] to achieve multi-bond, broadband ^{2}H–^{13}C polarization using an affordable ^{2}H radiofrequency field of ~50 kHz and a short contact time below 1.7 ms [70]. A rapid *trans*-gauche isomerization is identified in perdeuterated bacterial cellulose. This hydroxymethyl motion around the C5–C6 bond is absent in the interior glucan chains of cellulose but occurs to the surface chains as revealed by their motionally averaged C6–^{2}H quadrupolar couplings. In H/D exchanged *Arabidopsis* cell walls, $2D^{13}C$–^{2}H correlation spectra (Fig. 5c) have shown a mixed quadrupolar pattern that can be best deconvoluted into two components: the quadrupolar coupling constant is 50 kHz for the mobile matrix polysaccharides and 187 kHz for the rigid cellulose, which is a value approaching the hydrogen-bonded rigid deuteroxyl quadrupolar coupling (Fig. 5d). This robust method can be applied to evaluate the dynamics and water-accessible surface of carbohydrates in various organisms.

4.4. PRE: carbohydrate-ligand binding in cellular environment

In structural biology, carbohydrates are often treated as small ligands attached to large protein complexes, but this concept has been inverted in cell wall studies. In plant cell walls, functional proteins are usually present at low concentrations, but with the capabilities of perturbing polymer nexuses or chemically modifying/digesting certain structural motifs. For the β-expansins that cannot be produced recombinantly, the extracted proteins from grass pollens are tagged with paramagnetic Mn(II) labels via their solvent-accessible Cys residues (Fig. 5e), and mixed with the ^{13}C-labeled cell walls in maize [35]. Upon binding to expansin, the hemicellulose glucuronoarabinoxylan (GAX) has shown strong ^{1}H and ^{13}C Paramagnetic Relaxation Enhancement (PRE) effects (Fig. 5f and g), and its stiff and mobile fractions have become more rigid and dynamic, respectively. Therefore, β-expansins have released the connections between the highly substituted GAX (mobile) that forms the interfibrillar matrix and the rarely branched GAX (rigid) that are packed with cellulose microfibrils. The optimized protocols for incorporating paramagnetic sites and the PRE-enabled distance determination [71–74] have made it feasible for revealing the interactions between carbohydrates and many proteins or enzymes that contain carbohydrate-binding modules [75].

4.5. Natural-abundance DNP and database: accommodate the growing field

As an emerging technique, natural-abundance MAS-DNP has enabled the measurement of $2D^{13}C$–$^{13}C/^{15}N/^{1}H$ spectra on unlabeled biomolecules (Fig. 6a). When applied to organic molecules and small peptides, this technique could substantially facilitate NMR crystallography by enabling the determination of ^{13}N–^{13}C distance up to 7 Å and the measurement of ^{15}N–^{13}C correlation at natural isotope abundance [76–78]. Applications of this method to complicated biosystems allow us to extract long-range distance constraints in polyglutamine (polyQ) amyloid fibrils and nano-assemblies of cyclic peptides [77,79], validate imino acid-aromatic interactions in native collagens [80], and identify the compositional and conformational differences of cellulose, hemicellulose, and lignin in various plant species (cotton, rice, and poplar) [9,40,81]. These studies were conducted on medium magnetic fields, the 400 MHz/263 GHz or 600 MHz/395 GHz DNP instruments; due to the limited resolution, only highly ordered systems, such as cellulose microfibrils and amyloid fibrils, or a selected component within whole-cell sample could be studied. Because high-field DNP is still inefficient at this stage but has become a necessity for providing sufficient resolution for studying complex samples, the efforts trying to improve the polarization mechanism and radicals at high fields could substantially strengthen the capability of natural-abundance DNP [82–84].

A rate-limiting process associated with natural-abundance DNP is to interpret the large number of NMR-observables into structural information. We have recently demonstrated that a heatmap comparing the chemical shifts measured on the cotton cellulose and reported in literature allows us to quickly identify the relevant structures (Fig. 6b) [40]. This application benefits from the implementation of Complex Carbohydrates Magnetic Resonance Database (CCMRD) that supports the storage and sharing of information on chemical shifts, dynamics, and structure. CCMRD is freely available to the public at www.ccmrd.org and supports data deposition and data search by NMR chemical shifts, carbohydrate name, and compound class (Fig. 6c and d) [85]. By the time of this article, 450 compounds from plants, fungi, bacteria, algae, and engineered biomaterials are indexed by CCMRD, and this platform will accommodate the rapid expansion of the dataset and facilitate the development of statistics-based software [40]. My vision for carbohydrate ssNMR is to enable high-throughput and semi-automatic analysis of spectra and structure, which requires dedicated efforts in method and software development.

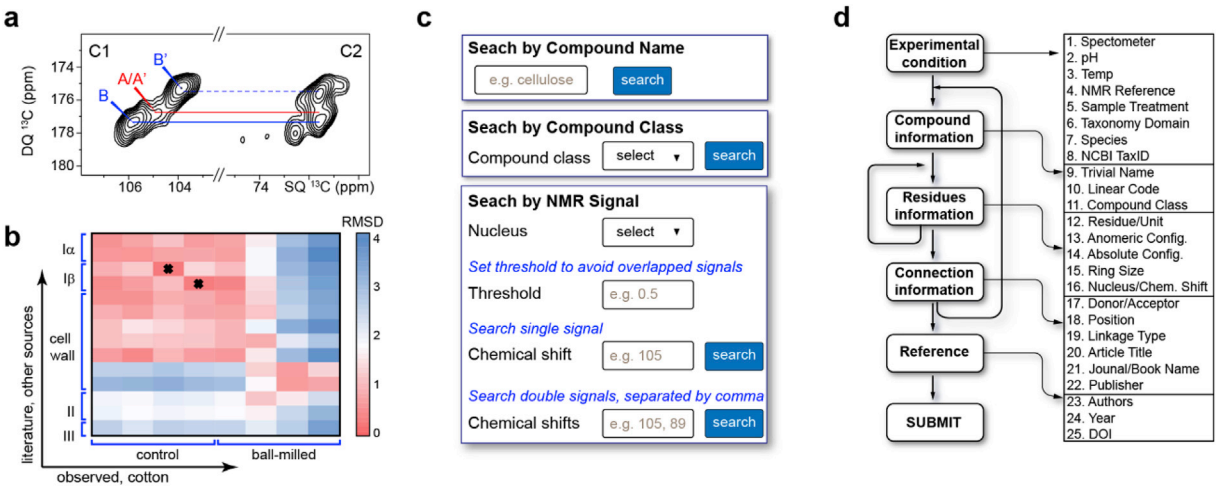

Fig. 6. Natural-abundance DNP of unlabeled material assisted by database development. **a**, Natural abundance 2D ^{13}C–^{13}C INADEQUATE spectrum of unlabeled cotton. A and A': glucose units in Iα cellulose allomorph; B and B': glucose units in Iβ allomorph. **b**, ^{13}C chemical shift RMSD map for comparisons between cotton and other cellulose sources. The color scale of RMSD (ppm) is shown. **c**, Search interface of CCMRD database that supports data search by compound name, class, and signal. **d**, Flowchart of data deposition and the 25 types of entries included for each compound. Adapted from reference [40,85] with copyright permission.

5. Concluding remarks

Solid-state NMR and DNP have demonstrated their unique capability in understanding the nanoscale assembly of fungal and plant cell walls. The rapid advances in NMR instrumentation and technology have made it possible to address biochemical and structural questions that were previously impossible to answer. The studies of plant and fungal cell walls, combined with the many investigations of other complex biosystems, such as the bacterial cell walls and biofilm, algal polysaccharides, and mammalian carbohydrates, have formed an emerging and unique research direction, which is of high significance to the development of biorenewable energy, biomedical therapies, and high-value products based on carbohydrate polymers.

Declaration of competing interest

The authors declare that they have no known competing financial interests or personal relationships that could have appeared to influence the work reported in this paper.

Acknowledgment

This work was supported by the National Science Foundation (CAREER award MCB-1942665) and the Center for Lignocellulose Structure and Formation, an Energy Frontier Research Center funded by the US Department of Energy, Office of Science, Basic Energy Sciences under award number DE-SC0001090.

References

[1] C. Somerville, H. Youngs, C. Taylor, S.C. Davis, S.P. Long, Feedstocks for lignocellulosic biofuels, Science 329 (2010) 790–792.
[2] F.C. Odds, A.J.P. Brown, N.A.R. Gow, Antifungal agents: mechanisms of action, Trends Microbiol. 11 (2003) 272–279.
[3] J.A. Romaniuk, L. Cegelski, Bacterial cell wall composition and the influence of antibiotics by cell-wall and whole-cell NMR, Phil. Trans. R. Soc. B 370 (2015).
[4] A. Kirui, M.C. Dickwella Widanage, F. Mentink-Vigier, P. Wang, X. Kang, T. Wang, Preparation of fungal and plant materials for structural elucidation using dynamic nuclear polarization solid-state NMR, J. Vis. Exp. 144 (2019), e59152.
[5] M. Dick-Perez, Y.A. Zhang, J. Hayes, A. Salazar, O.A. Zabotina, M. Hong, Structure and interactions of plant cell wall polysaccharides by two- and three-dimensional magic-angle-spinning solid-state NMR, Biochemistry 50 (2011) 989–1000.
[6] T. Wang, O. Zabotina, M. Hong, Pectin-cellulose interactions in the *Arabidopsis* primary cell wall from two-dimensional magic-angle-spinning solid-state nuclear magnetic resonance, Biochemistry 51 (2012) 9846–9856.
[7] T. Wang, A. Salazar, O.A. Zabotina, M. Hong, Structure and dynamics of *Brachypodium* primary cell wall polysaccharides from two-dimensional ^{13}C solid-state nuclear magnetic resonance spectroscopy, Biochemistry 53 (2014) 2840–2854.
[8] X. Kang, A. Kirui, M.C. Dickwella Widanage, F. Mentink-Vigier, D.J. Cosgrove, T. Wang, Lignin-polysaccharide interactions in plant secondary cell walls revealed by solid-state NMR, Nat. Commun. 10 (2019) 347.
[9] F.A. Perras, H. Luo, X. Zhang, N.S. Mosier, M. Pruski, M.M. Abu-Omar, Atomic-Level structure characterization of biomass pre- and post-lignin treatment by dynamic nuclear polarization-enhanced solid-state NMR, J. Phys. Chem. A 121 (2017) 623–630.
[10] T.J. Simmons, J.C. Mortimer, O.D. Bernardinelli, A.C. Poppler, S.P. Brown, E.R. deAzevedo, R. Dupree, P. Dupree, Folding of xylan onto cellulose fibrils in plant cell walls revealed by solid-state NMR, Nat. Commun. 7 (2016) 13902.
[11] N.J. Grantham, J. Wurman-Rodrich, O.M. Terrett, J.J. Lyczakowski, K. Stott, D. Iuga, T.J. Simmons, M. Durand-Tardif, S.P. Brown, R. Dupree, M. Busse-Wicher, P. Dupree, An even pattern of xylan substitution is critical for interaction with cellulose in plant cell walls, Nat. Plants 3 (2017) 859–865.
[12] R. Dupree, T.J. Simmons, J.C. Mortimer, D. Patel, D. Iuga, S.P. Brown, P. Dupree, Probing the molecular architecture of Arabidopsis thaliana secondary cell walls using two- and three-dimensional ^{13}C solid state nuclear magnetic resonance spectroscopy, Biochemistry 54 (2015) 2335–2345.
[13] O.M. Terrett, J.J. Lyczakowski, L. Yu, D. Iuga, W.T. Franks, S.P. Brown, R. Dupree, P. Dupree, Molecular architecture of softwood revealed by solid-state NMR, Nat. Commun. 10 (2019) 4978.
[14] J. Viger-Gravel, W. Lan, A.C. Pinon, P. Berruyer, L. Emsley, M. Barder, J. Luterbacher, Topology of pretreated wood fibers using dynamic nuclear polarization, J. Phys. Chem. C 123 (2019) 30407–30415.
[15] X. Kang, A. Kirui, A. Muszynski, M.C.D. Widanage, A. Chen, P. Azadi, P. Wang, F. Mentink-Vigier, T. Wang, Molecular architecture of fungal cell walls revealed by solid-state NMR, Nat. Commun. 9 (2018) 2747.
[16] S. Chatterjee, R. Prados-Rosales, S. Frases, B. Itin, A. Casadevall, R.E. Stark, Using solid-state NMR to monitor the molecular consequences of Cryptococcus neoformans melanization with different catecholamine precursors, Biochemistry 51 (2012) 6080–6088.
[17] S. Chatterjee, R. Prados-Rosales, B. Itin, A. Casadevall, R.E. Stark, Solid-state NMR reveals the carbon-based molecular architecture of Cryptococcus neoformans fungal eumelanins in the cell wall, J. Biol. Chem. 290 (2015) 13779–13790.
[18] R. Nygaard, J.A.H. Romaniuk, D.M. Rice, L. Cegelski, Spectral snapshots of bacterial cell-wall composition and the influence of antibiotics by whole-cell NMR, Biophys. J. 108 (2015) 1380–1389.
[19] H. Takahashi, I. Ayala, M. Bardet, G. De Paepe, J.P. Simorre, S. Hediger, Solid-state NMR on bacterial cells: selective cell wall signal enhancement and resolution improvement using dynamic nuclear polarization, J. Am. Chem. Soc. 135 (2013) 5105–5110.
[20] T. Kern, M. Giffard, S. Hediger, A. Amoroso, C. Giustini, N.K. Bui, B. Joris, C. Bougault, W. Vollmer, J.P. Simorre, Dynamics characterization of fully hydrated bacterial cell walls by solid-state NMR: evidence for cooperative binding of metal ions, J. Am. Chem. Soc. 132 (2010) 10911–10919.
[21] W. Thongsomboon, D.O. Serra, A. Possling, C. Hadjineophytou, R. Hengge, L. Cegelski, Phosphoethanolamine cellulose: a naturally produced chemically modified cellulose, Science 359 (2018) 334–338.
[22] A.A. Arnold, J.P. Bourgouin, B. Genard, D.E. Warschawski, R. Tremblay, I. Marcotte, Whole cell solid-state NMR study of Chlamydomonas reinhardtii microalgae, J. Biomol. NMR 70 (2018) 123–131.

[23] T. Wang, M. Hong, Solid-state NMR investigations of cellulose structure and interactions with matrix polysaccharides in plant primary cell walls, J. Exp. Bot. 67 (2016) 503–514.
[24] T. Wang, P. Phyo, M. Hong, Multidimensional solid-state NMR spectroscopy of plant cell walls, Solid State Nucl. Magn. Reson. 78 (2016) 56–63.
[25] N.C. Carpita, Structure and biogenesis of the cell walls of grasses, Annu. Rev. Plant Physiol. 47 (1996) 445–476.
[26] N.C. Carpita, D.M. Gibeaut, Structural models of primary cell walls in flowering plants: consistency of molecular structure with the physical properties of the walls during growth, Plant J. 3 (1993) 1–30.
[27] T. Wang, J.K. Williams, K. Schmidt-Rohr, M. Hong, Relaxation-compensated difference spin diffusion NMR for detecting ^{13}C-^{13}C long-range correlations in proteins and polysaccharides, J. Biomol. NMR 61 (2015) 97–107.
[28] T. Wang, Y.B. Park, D.J. Cosgrove, M. Hong, Cellulose-pectin spatial contacts are inherent to never-dried Arabidopsis thaliana primary cell walls: evidence from solid-state NMR, Plant Physiol. 168 (2015) 871–884.
[29] P.B. White, T. Wang, Y.B. Park, D.J. Cosgrove, M. Hong, Water-polysaccharide interactions in the primary cell wall of *Arabidopsis thaliana* from polarization transfer solid-state NMR, J. Am. Chem. Soc. 136 (2014) 10399–10409.
[30] M. Dick-Perez, T. Wang, A. Salazar, O.A. Zabotina, M. Hong, Multidimensional solid-state NMR studies of the structure and dynamics of pectic polysaccharides in uniformly ^{13}C-labeled Arabidopsis primary cell walls, Magn. Reson. Chem. 50 (2012) 539–550.
[31] P. Phyo, T. Wang, S.N. Kiemle, H. O'Neill, S.V. Pingali, M. Hong, D.J. Cosgrove, Gradients in wall mechanics and polysaccharides along growing inflorescence stems, Plant Physiol. 175 (2017) 1593–1607.
[32] P. Phyo, T. Wang, C.W. Xiao, C.T. Anderson, M. Hong, Effects of pectin molecular weight changes on the structure, dynamics, and polysaccharide interactions of primary cell walls of Arabidopsis thaliana: insights from solid-state NMR, Biomacromolecules 18 (2017) 2937–2950.
[33] P. Phyo, Y. Gu, M. Hong, Impact of acidic pH on plant cell wall polysaccharide structure and dynamics: insights into the mechanism of acid growth in plants from solid-state NMR, Cellulose 26 (2019) 291–304.
[34] T. Wang, Y.B. Park, M.A. Caporini, M. Rosay, L.H. Zhong, D.J. Cosgrove, M. Hong, Sensitivity-enhanced solid-state NMR detection of expansin's target in plant cell walls, Proc. Natl. Acad. Sci. U.S.A. 110 (2013) 16444–16449.
[35] T. Wang, Y.N. Chen, A. Tabuchi, D.J. Cosgrove, M. Hong, The target of beta-expansin EXPB1 in maize cell walls from binding and solid-state NMR studies, Plant Physiol. 172 (2016) 2107–2119.
[36] D.J. Cosgrove, Loosening of plant cell walls by expansins, Nature 407 (2000) 321–326.
[37] T. Wang, H. Yang, J.D. Kubicki, M. Hong, Cellulose structural polymorphism in plant primary cell walls investigated by high-field 2D solid-state NMR spectroscopy and density functional theory calculations, Biomacromolecules 17 (2016) 2210–2222.
[38] P. Phyo, T. Wang, Y. Yang, H. O'Neill, M. Hong, Direct determination of hydroxymethyl conformations of plant cell wall cellulose using ^{1}H polarization transfer solid-state NMR, Biomacromolecules 19 (2018) 1485–1497.
[39] H. Yang, T. Wang, D. Oehme, L. Petridis, M. Hong, J.D. Kubicki, Structural factors affecting ^{13}C NMR chemical shifts of cellulose: a computational study, Cellulose 25 (2018) 23–36.
[40] A. Kirui, Z. Ling, X. Kang, M.C. Dickwella Widanage, F. Mentink-Vigier, A.D. French, T. Wang, Atomic resolution of cotton cellulose structure enabled by dynamic nuclear polarization solid-state NMR, Cellulose 26 (2019) 329–339.
[41] D.J. Cosgrove, M.C. Jarvis, Comparative structure and biomechanics of plant primary and secondary cell walls, Front. Plant Sci. 3 (2012).
[42] G. De Paepe, J.R. Lewandowski, A. Loquet, A. Bockmann, R.G. Griffin, Proton assisted recoupling and protein structure determination, J. Chem. Phys. 129 (2008).
[43] J.P. Latge, The cell wall: a carbohydrate armour for the fungal cell, Mol. Microbiol. 66 (2007) 279–290.
[44] P.D. Stahl, R.A.B. Ezekowitz, The mannose receptor is a pattern recognition receptor involved in host defense, Curr. Opin. Immunol. 10 (1998) 50–55.
[45] L.B. Andreas, K. Jaudzems, J. Stanek, D. Lalli, A. Bertarello, T. Le Marchand, D. Cala-De Paepe, S. Kotelovica, I. Akopjana, B. Knott, S. Wegner, F. Engelke, A. Lesage, L. Emsley, K. Tars, T. Herrmann, G. Pintacuda, Structure of fully protonated proteins by proton-detected magic-angle spinning NMR, Proc. Natl. Acad. Sci. U.S.A. 113 (2016) 9187–9192.
[46] I. Bertini, L. Emsley, M. Lelli, C. Luchinat, J.F. Mao, G. Pintacuda, Ultrafast MAS solid-state NMR permits extensive ^{13}C and ^{1}H detection in paramagnetic metalloproteins, J. Am. Chem. Soc. 132 (2010) 5558–5559.
[47] D.H. Zhou, G. Shah, M. Cormos, C. Mullen, D. Sandoz, C.M. Rienstra, Proton-detected solid-state NMR Spectroscopy of fully protonated proteins at 40 kHz magic-angle spinning, J. Am. Chem. Soc. 129 (2007) 11791–11801.
[48] J. Struppe, C.M. Quinn, M.M. Lu, M.Z. Wang, G.J. Hou, X.Y. Lu, J. Kraus, L.B. Andreas, J. Stanek, D. Lalli, A. Lesage, G. Pintacuda, W. Maas, A.M. Gronenborn, T. Polenova, Expanding the horizons for structural analysis of fully protonated protein assemblies by NMR spectroscopy at MAS frequencies above 100 kHz, Solid State Nucl, Magnes. Res. 87 (2017) 117–125.
[49] B. Elena, A. Lesage, S. Steuernagel, A. Bockmann, L. Emsley, Proton to carbon-13 INEPT in solid-state NMR spectroscopy, J. Am. Chem. Soc. 127 (2005) 17296–17302.
[50] V. Agarwal, B. Reif, Residual methyl protonation in perdeuterated proteins for multi-dimensional correlation experiments in MAS solid-state NMR spectroscopy, J. Magn. Reson. 194 (2008) 16–24.
[51] M. Baldus, B.H. Meier, Total correlation spectroscopy in the solid state. The use of scalar couplings to determine the through-bond connectivity, J. Magn. Reson. A 121 (1996) 65–69.
[52] P. Phyo, M. Hong, Fast MAS ^{1}H-^{13}C correlation NMR for structural investigations of plant cell walls, J. Biomol. NMR 73 (2019) 661–674.
[53] C. Bougault, I. Ayala, W. Vollmer, J.P. Simorre, P. Schanda, Studying intact bacterial peptidoglycan by proton-detected NMR spectroscopy at 100 kHz MAS frequency, J. Struct. Biol. 206 (2019) 66–72.
[54] P. Schanda, S. Triboulet, C. Laguri, C.M. Bougault, I. Ayala, M. Callon, M. Arthur, J.P. Simorre, Atomic model of a cell-wall cross-linking enzyme in complex with an intact bacterial peptidoglycan, J. Am. Chem. Soc. 136 (2014) 17852–17860.
[55] M. Roos, V.S. Mandala, M. Hong, Determination of long-range distances by fast magic-angle-spinning radiofrequency-driven ^{19}F-^{19}F dipolar recoupling NMR, J. Phys. Chem. B 122 (2018) 9302–9313.
[56] A.A. Shcherbakov, V.S. Mandala, M. Hong, High-sensitivity detection of nanometer 1H-19F distances for protein structure determination by H-1-Detected fast MAS NMR, J. Phys. Chem. B 123 (2019) 4387–4391.
[57] M. Wang, M. Lu, M.P. Fritz, C.M. Quinn, I.L. Byeon, C.H. Byeon, J. Struppe, W. Maas, A.M. Gronenborn, T. Polenova, Fast magic-angle spinning ^{19}F NMR spectroscopy of HIV-1 capsid protein assemblies, Angew. Chem., Int. Ed. Engl. 57 (2018) 16375–16379.
[58] R.A. Fry, N. Tsomaia, C.G. Pantano, K.T. Mueller, ^{19}F MAS NMR quantification of accessible hydroxyl sites on fiberglass surfaces, J. Am. Chem. Soc. 125 (2003) 2378–2379.
[59] B.H. Meier, Polarization transfer and spin diffusion in solid-state NMR, Adv. Magn. Opt. Reson. 18 (1994) 1–116.
[60] Z.H. Gan, I. Hung, X.L. Wang, J. Paulino, G. Wu, I.M. Litvak, P.L. Gor'kov, W.W. Brey, P. Lendi, J.L. Schiano, M.D. Bird, L.R. Dixon, J. Toth, G.S. Boebinger, T.A. Cross, NMR spectroscopy up to 35.2 T using a series-connected hybrid magnet, J. Magn. Reson. 284 (2017) 125–136.
[61] E.G. Keeler, V.K. Michaelis, M.T. Colvin, I. Hung, P.L. Gor'kov, T.A. Cross, Z.H. Gan, R.G. Griffin, ^{17}O MAS NMR correlation spectroscopy at high magnetic fields, J. Am. Chem. Soc. 139 (2017) 17953–17963.
[62] T. Gullion, Measurement of dipolar interactions between spin-1/2 and quadrupolar nuclei by rotational-echo, adiabatic-passage, double-resonance nmr, Chem. Phys. Lett. 246 (1995) 325–330.
[63] T.H. Sefzik, J.B. Houseknecht, T.M. Clark, S. Prasad, T.L. Lowary, Z. Gan, P.J. Grandinetti, Solid-state ^{17}O NMR in carbohydrates, Chem. Phys. Lett. 434 (2007) 312–315.
[64] G.L. Jiao, G.L. Yu, J.Z. Zhang, H.S. Ewart, Chemical structures and bioactivities of sulfated polysaccharides from marine algae, Mar. Drugs 9 (2011) 196–223.
[65] W.J. Zhang, B. Falcon, A.G. Murzin, J. Fan, R.A. Crowther, M. Goedert, S.H.W. Scheres, Heparin-induced tau filaments are polymorphic and differ from those in Alzheimer's and Pick's diseases, Elife 8 (2019).
[66] T. Wang, M. Hong, Structure and Dynamics of Polysaccharidesin Plant Cell Walls from Solid-State NMR, Royal Society of Chemistry, 2017.
[67] X.L. Yao, K. Schmidt-Rohr, M. Hong, Medium- and long-distance ^{1}H-^{13}C heteronuclear correlation NMR in solids, J. Magn. Reson. 149 (2001) 139–143.
[68] S. Jain, M. Bjerring, N.C. Nielsen, Efficient and robust heteronuclear cross-polarization for high-speed-spinning biological solid-state NMR spectroscopy, J. Phys. Chem. Lett. 3 (2012) 703–708.
[69] D. Wei, U. Akbey, B. Paaske, H. Oschkinat, B. Reif, M. Bjerring, N.C. Nielsen, Optimal ^{2}H rf pulses and ^{2}H-^{13}C cross-polarization methods for solid-state ^{2}H MAS NMR of perdeuterated proteins, J. Phys. Chem. Lett. 2 (2011) 1289–1294.
[70] M.D. Gelenter, T. Wang, S.Y. Liao, H. O'Neill, M. Hong, ^{2}H-^{13}C correlation solid-state NMR for investigating dynamics and water accessibilities of proteins and carbohydrates, J. Biol. NMR 68 (2017) 257–270.
[71] C.P. Jaroniec, Structural studies of proteins by paramagnetic solid-state NMR spectroscopy, J. Magn. Reson. 253 (2015) 50–59.
[72] I. Sengupta, P.S. Nadaud, J.J. Helmus, C.D. Schwieters, C.P. Jaroniec, Protein fold determined by paramagnetic magic-angle spinning solid-state NMR spectroscopy, Nat. Chem. 4 (2012) 410–417.
[73] J. Iwahara, G.M. Clore, Detecting transient intermediates in macromolecular binding by paramagnetic NMR, Nature 440 (2006) 1227–1230.
[74] I. Bertini, C. Luchinat, G. Parigi, R. Pierattelli, NMR spectroscopy of paramagnetic metalloproteins, Chembiochem 6 (2005) 1536–1549.
[75] A.B. Boraston, D.N. Bolam, H.J. Gilbert, G.J. Davies, Carbohydrate-binding modules: fine-tuning polysaccharide recognition, Biochem. J. 382 (2004) 769–781.
[76] K. Marker, M. Pingret, J.M. Mouesca, D. Gasparutto, S. Hediger, G. De Paepe, A new tool for NMR crystallography: complete $^{13}C/^{15}N$ assignment of organic molecules at natural isotopic abundance using DNP-enhanced solid-state NMR, J. Am. Chem. Soc. 137 (2015) 13796–13799.
[77] K. Marker, S. Paul, C. Fernandez-de-Alba, D. Lee, J.M. Mouesca, S. Hediger, G. De Paepe, Welcoming natural isotopic abundance in solid-state NMR: probing π-stacking and supramolecular structure of organic nanoassemblies using DNP, Chem. Sci. 8 (2017) 974–987.
[78] R.A. Olsen, J. Struppe, D.W. Elliott, R.J. Thomas, L.J. Mueller, Through-bond ^{13}C-^{13}C correlation at the natural abundance level: refining dynamic regions in the crystal structure of vitamin-D-3 with solid-state NMR, J. Am. Chem. Soc. 125 (2003) 11784–11785.
[79] A.N. Smith, K. Marker, T. Piretra, J.C. Boatz, I. Matlahov, R. Kodali, S. Hediger, P.C.A. van der Wel, G. De Paepe, Structural fingerprinting of protein aggregates by dynamic nuclear polarization-enhanced solid-state NMR at natural isotopic abundance, J. Am. Chem. Soc. 140 (2018) 14576–14580.

[80] C. Singh, R.K. Rai, F. Aussenac, N. Sinha, Direct evidence of imino acid-aromatic interactions in native collagen protein by DNP-enhanced solid-state NMR spectroscopy, J. Phys. Chem. Lett. 5 (2014) 4044–4048.
[81] L. Zhang, C. Gao, F. Mentink-Vigier, L. Tang, D. Zhang, S. Wang, S. Cao, Z. Xu, X. Liu, T. Wang, Y. Zhou, B. Zhang, Arabinosyl deacetylase modulates the arabinoxylan acetylation profile and secondary wall formation, Plant Cell 31 (2019) 1113–1126.
[82] G. Mathies, M.A. Caporini, V.K. Michaelis, Y.P. Liu, K.N. Hu, D. Mance, J.L. Zweier, M. Rosay, M. Baldus, R.G. Griffin, Efficient dynamic nuclear polarization at 800 MHz/527 GHz with trityl-nitroxide biradicals, Angew. Chem. Int. Ed. 54 (2015) 11770–11774.
[83] K. Jaudzems, A. Bertarello, S.R. Chaudhari, A. Pica, D. Cala-De Paepe, E. Barbet-Massin, A.J. Pell, I. Akopjana, S. Kotelovica, D. Gajan, O. Ouari, K. Tars, G. Pintacuda, A. Lesage, Dynamic nuclear polarization-enhanced biomolecular NMR spectroscopy at high magnetic field with fast magic-angle spinning, Angew. Chem. Int. Ed. 57 (2018) 7458–7462.
[84] F. Mentink-Vigier, I. Marin-Montesinos, A.P. Jagtap, T. Halbritter, J. van Tol, S. Hediger, D. Lee, S.T. Sigurdsson, G. De Paepe, Computationally assisted design of polarizing agents for dynamic nuclear polarization enhanced NMR: the AsymPol family, J. Am. Chem. Soc. 140 (2018) 11013–11019.
[85] X. Kang, W. Zhao, M.C. Dickwella Widanage, A. Kirui, U. Ozdenvar, T. Wang, CCMRD: a solid-state NMR database for complex carbohydrates, J. Biomol. NMR (2020), https://doi.org/10.1007/s10858-020-00304-2. In press.

Wancheng Zhao obtained his B.S. degree (Chemistry) from Jilin University in China in 2011. He obtained his M.S. degree (Chemistry) at Renmin University, China in 2017, under the supervision of Dr. Tiancheng Mu. His PhD research at Louisiana State University focuses on database development and the elucidation of plant cell wall structure using natural-abundance DNP.

Liyanage D. Fernando obtained her B.S. degree at University of Colombo in Sri Lanka in 2017. Her PhD research at Louisiana State University, supervised by Dr. Tuo Wang, focuses on the employment of solid-state NMR methods to understand the structural diversity of carbohydrates in fungal pathogens.

Alex Kirui obtained his B.S. degree from The Technical University of Kenya in Nairobi, Kenya in 2015. His PhD research at Louisiana State University, supervised by Dr. Tuo Wang, focuses on the development and application of solid-state NMR and natural-abundance DNP methods to elucidate the structure and dynamics of plant cell walls.

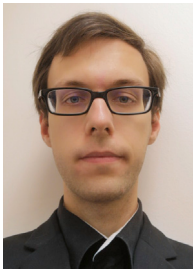

Dr. Fabien Deligey graduated in physics at Université de Lorraine, France, where he also obtained his PhD degree in 2019, under the supervision of Dr. Sabine **Bouguet**-Bonnet and Axel Gansmülle. He employed solid-state NMR to characterize nanoparticles and hybrid materials designed for drug delivery. He is now a postdoctoral associate in Tuo Wang group at Louisiana State University conducting solid-state NMR and DNP research on a variety of biomaterials

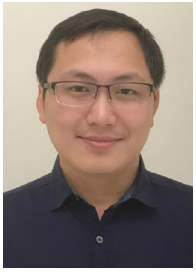

Dr. Tuo Wang started his graduate research at Iowa State University in 2010 and moved to Massachusetts Institute of Technology (MIT) in 2014. He received his **PhD** in Physical Chemistry from MIT in 2016 (supervised by Dr. Mei Hong). He continued at Mei Hong's group for postdoctoral training and joined the Chemistry Department at Louisiana State University in 2017. He focuses on the structural elucidation of complex carbohydrates and other biomolecules.